Acta Neuropathol (2006) 112:127–137
DOI 10.1007/s00401-006-0086-4

ORIGINAL PAPER

Effect of 6-hydroxydopamine treatment on kynurenine aminotransferase-I (KAT-I) immunoreactivity of neurons and glial cells in the rat substantia nigra

Elizabeth Knyihár-Csillik · Zoltan Chadaide · András Mihály · Beata Krisztin-Péva · Robert Fenyő · László Vécsei

Received: 29 December 2005 / Revised: 11 May 2006 / Accepted: 11 May 2006 / Published online: 21 June 2006

Abstract Parkinson's disease (PD), a progressive neurodegenerative disorder, is characterized by a preferential loss of dopaminergic neurons in the substantia nigra pars compacta (SNPC). Neurons in the SNPC are known to express tyrosine hydroxylase (TH); therefore, in a commonly used PD model, 6-hydroxydopamine (6-OHDA), a selective catecholamine neurotoxin, induces neuronal death in SNPC. We have shown with immunohistochemical techniques that kynurenine aminotransferase-I (KAT-I), the enzyme taking part in the formation of kynurenic acid (KYNA)—the only known endogenous selective NMDA receptor antagonist and a potent neuroprotective agent—is also expressed in the rat SNPC. We found that KAT-I and TH co-exist in the very same neurons of SNPC and that 6-OHDA injected into the lateral ventricle produced loss of the majority of nigral neurons. Densitometric analysis proved that, in consequence of 6-OHDA treatment, not only TH but also KAT-I immunoreactivity diminished considerably in the remaining SNPC neurons. Astrocytes in the substantia nigra were found to express KAT-I under normal conditions; the amount of this enzyme increased after administration of 6-OHDA, whereas microglial cells became KAT-I immunoreactive only after 6-OHDA treatment. Since intrinsic KYNA in SNPC neurons is perceptibly insufficient to protect them from the deleterious effect of 6-OHDA, it is hypothesized that biochemical approaches which increase KYNA content of the central nervous system might prevent the deleterious effect of 6-OHDA and, supposedly, also the neuronal degradation characterizing PD.

Keywords 6-Hydroxydopamine · Immunocytochemistry · Kynurenine aminotransferase · Parkinson's disease · Substantia nigra

E. Knyihár-Csillik (✉) · Z. Chadaide · L. Vécsei
Department of Neurology, Albert Szent-Györgyi Medical and Pharmaceutical Center, University of Szeged, 6701 Szeged, Hungary
e-mail: knyihar@nepsy.szote.u-szeged.hu

A. Mihály · B. Krisztin-Péva · R. Fenyő
Department of Anatomy, Albert Szent-Györgyi Medical and Pharmaceutical Center, University of Szeged, 6701 Szeged, Hungary

L. Vécsei
Neurology Research Group, Hungarian Academy of Sciences, University of Szeged, Szeged, Hungary

Introduction

The molecular pathways involved in Parkinson's disease (PD) have been studied in a wide variety of experimental models designed to mimic specific pathogenic events of the human disease. In the most widely used model of PD in rats, intracerebral administration of the catecholamine-cell-specific neurotoxin 6-hydroxydopamine (6-OHDA) was used, injected into different parts of the nigrostriatal pathway, such as the striatum, the medial forebrain bundle, and the substantia nigra pars compacta (SNPC). Such models may help define cellular factors of cell death which are critical for nigral degeneration [2, 6, 12, 14, 15, 34].

Although the etiology of the cellular mechanisms underlying PD is unknown, several factors, such as environmental and genetic elements, are known to induce relatively selective dopaminergic cell death in

the substantia nigra (SN) which is accompanied by characteristic clinical features of PD. Thus, according to Barkats et al. [1], the neurotoxin 6-OHDA may cause dopaminergic cell death via free radical mechanisms. These investigations underline the major contribution of superoxide in the process of dopaminergic cell death induced by 6-OHDA. This has been linked with the selective accumulation of iron in the Parkinsonian SN and iron-catalyzed free radical formation. Iron-induced lipid peroxidation has been proposed as a possible cause of nigral cell death [13].

Endogenous excitotoxins that act on the receptors of cerebral excitatory amino acids may also play important roles in the pathogenesis of excitotoxic brain diseases: activation of excitatory amino acid receptors results in selective neuronal death characteristic of these disorders, including PD [4].

Kynurenic acid (KYNA) is a selective antagonist at the strychnine-insensitive glycine site of the NMDA receptor [20, 35]; therefore, it is considered to be a potent neuroprotective agent [28]. KYNA is produced from its biological precursor, L-kynurenine, by the enzyme kynurenine aminotransferase (KAT), and plays an important role in the tryptophan metabolism of the central nervous system (CNS) [38]. According to the biochemical analysis of tissue homogenates, KAT activity is present in rat and human brains [11, 29, 30]. Two distinctly different isoforms of KAT appear to be responsible for the synthesis of KYNA under physiological conditions. One of these, KAT-I, is a soluble enzyme; KAT-I antibodies were raised by Okuno and co-workers [29] and were used in the immunohistochemical investigations [7, 18, 32]. Another enzyme, KAT-II, was identified by Northern blot mRNA analysis in the human brain [30]. Immunohistochemical studies using anti-KAT-I antibody localized KAT-I immunoreactive (IR) mainly in the astrocytes of forebrain structures [7, 22]. L-Kynurenine is known to cross the blood–brain barrier; it can be transaminated to KYNA, the excitatory amino acid receptor antagonist, by the enzyme activity of KAT, known to be primarily located in glia [30]. Furthermore, it has been shown that glial cells possess the uptake mechanisms for L-kynurenine, and can release KYNA [36, 37]. At the same time, KAT-I IR was observed also in several nerve cells [30, 32], mainly in the medulla oblongata and spinal cord [18].

In the course of our earlier investigations, we studied the effects of sodium azide [22], 3-nitropropionic acid [5], and 1-methyl-4-phenyl-1,2,3,6-tetrahydropyridine (MPTP) treatment on KAT-I of various nerve and glial

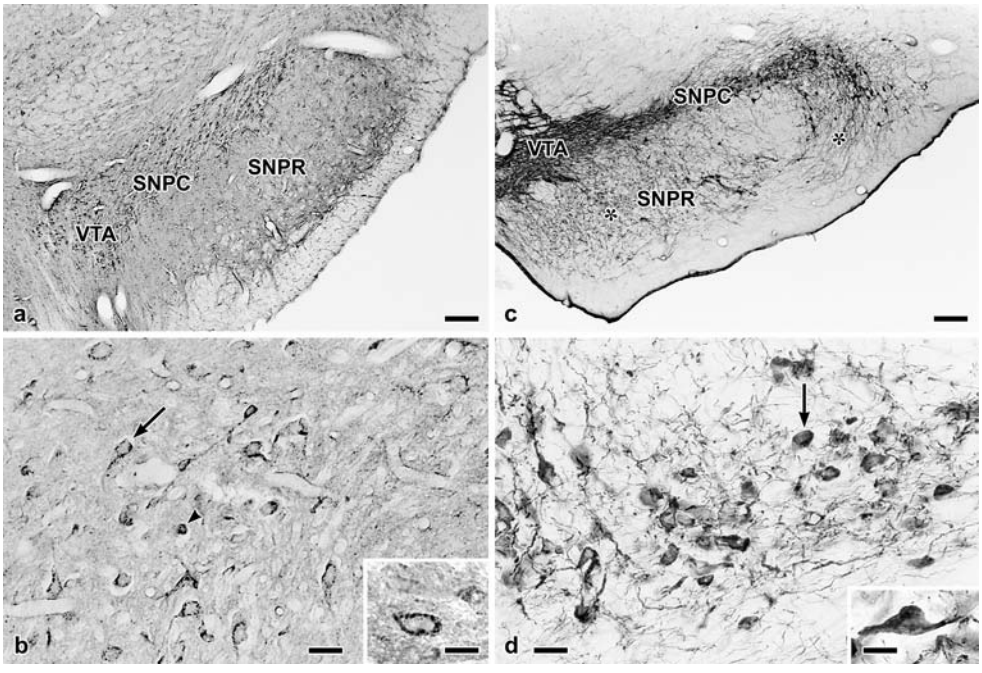

Fig. 1 Normal distribution of *KAT-I* and *TH* in the *SN*. **a** *KAT-I IR* outlines the *SNPC* (scale bar, 100 μm). **b** Under high power, the granular localization of the *KAT-I IR* is conspicuous (*arrow*). *KAT-I* granules in the perikaryon surround the nucleus; granules are also present in the proximal parts of the cell processes (inset: scale bar, 10 μm). The glial cells additionally exert *KAT-I IR* (*arrowhead*) (scale bar, 40 μm). Inset: *KAT-I IR* neuron at high power (scale bar, 10 μm). **c** The *TH IR* outlines the *SNPC*. The *SNPR* is almost totally occupied by *TH IR* processes of dopaminergic neurons (*asterisks*) (scale bar, 100 μm). **d** The localization of *TH* in the neuronal cytoplasm is homogeneous (*arrow*), as seen at high power (scale bar, 40 μm). The *TH* staining of the dopaminergic neurons is especially striking in the inset (scale bar, 10 μm)

cells of the CNS [21]. Specifically, we found that in the SN, where KAT-I and tyrosine hydroxylase (TH) co-exist in neuronal cytoplasms [21], MPTP treatment of mice resulted in decrease of number and optical density of KAT-I IR neurons, whereas KAT-I IR of glial cells was increased. Since most of the relevant studies, using 6-OHDA as a specific neurotoxin of dopaminergic neurons, were performed on the SN of rats, we decided to investigate, with immunocytochemical methods, whether KAT-I is also present in the nerve and glial cells of the SNPC of the rat, similarly to those of the mouse. Another question related to the possible effect of the 6-OHDA-induced nerve cell degeneration upon KAT-I. Finally, we investigated the distribution of KAT-I in the glial cells of the SN under normal conditions and after 6-OHDA administration.

Experimental procedures

Animals

Investigations were performed on 35 adult male albino rats (*Rattus norvegicus albus*), Wistar strain, 250-g body weight. Care of the animals complied with the guidelines of the Hungarian Ministry of Welfare; experiments were carried out in accordance with the European Communities Council Directive (24 November 1986; 86/609/EEC). The animals were divided into six groups: one group was the absolute control and the second group was injected into the left lateral ventricle with physiologic saline; four groups of rats were stereotactically injected into the left lateral ventricle with graded doses of 6-OHDA, ranging from 40 to 800 μg/kg. For stereotactic surgery, 6-OHDA (Sigma-Aldrich, Steinheim, Germany) was dissolved in PBS. Stereotactic injections were performed under pentobarbital anesthesia. Coordinates of the injections were as follows: AP: -0.8 mm from the bregma, ML: −1.4 mm from the sutura sagittalis, and V (depth): 4.0 mm from the skull [31]. Rats were unilaterally injected into the left lateral ventricle using a Hamilton microsyringe. The needle was left in place for an additional 2 min and then slowly withdrawn. The correct positioning of the cannula was checked by dissection of the brain at the end of the experiment. After a survival time of 23 days, rats were deeply anesthetized with chloral hydrate (4 g/kg i.p.) and transcardially perfused with a flush of 40 ml of 0.1 M PBS (pH 7.4), which was followed by 500 ml of PLP fixative, consisting of paraformaldehyde, lysine, and periodate, buffered to pH 7.4 with 0.4 M PBS [25]. Brains were removed in toto, both sides of the SN were excised and postfixed in the same fixative for 3 h at 4°C. The samples were processed in a graded series of sucrose (10, 20, and 30%) dissolved in PBS, surrounded by Tissue-Tek embedding medium (Miles, Diagnostics Division, Elkhart, IN, USA) and frozen in the chamber of the cryostat at −22°C. Transverse consecutive sections, 30 μm thick, were obtained from the entire SN.

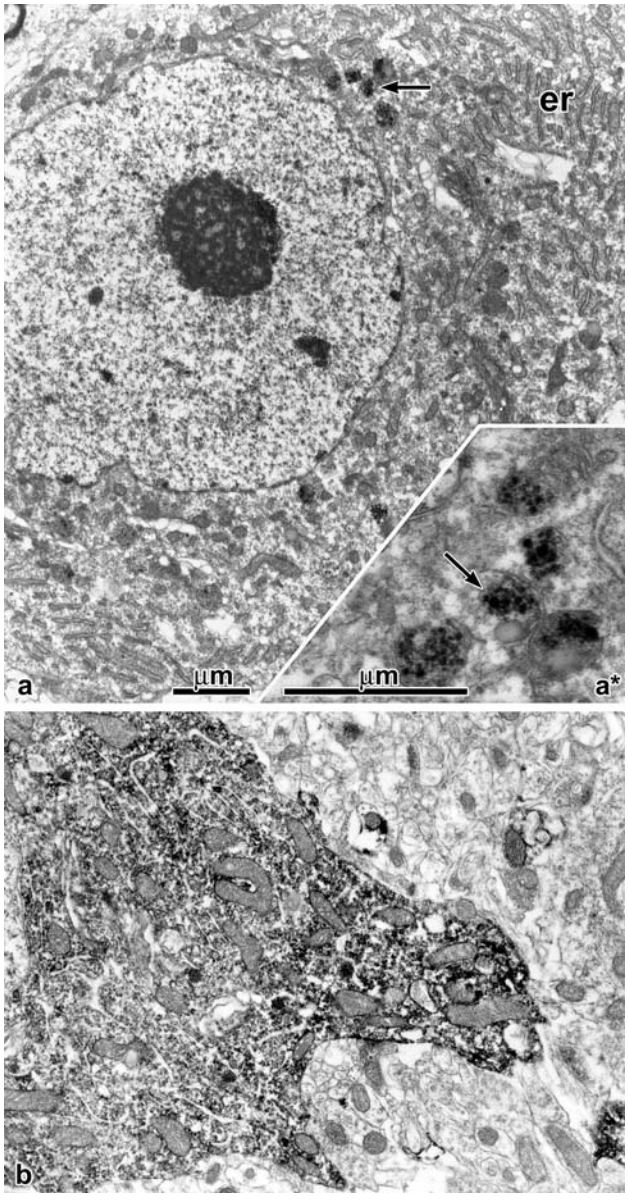

Fig. 2 Electron microscopy of *KAT-I IR* in the nerve cells in the *SNPC*. **a** In the perikaryon of a normal nerve cell, the *KAT-I IR* appears in granular form (*arrows*), surrounding the nucleus (*er*: endoplasmic reticulum). **a*** The granules indicated by *arrows* in **a**, at higher magnification. Some of the "granules" correspond to multivesicular bodies. **b** *TH IR* in the perikaryon of a normal neuron. The end product of the *IR* is attached to the surfaces of ribosomes (*arrows*). Magnification identical to that in **a**

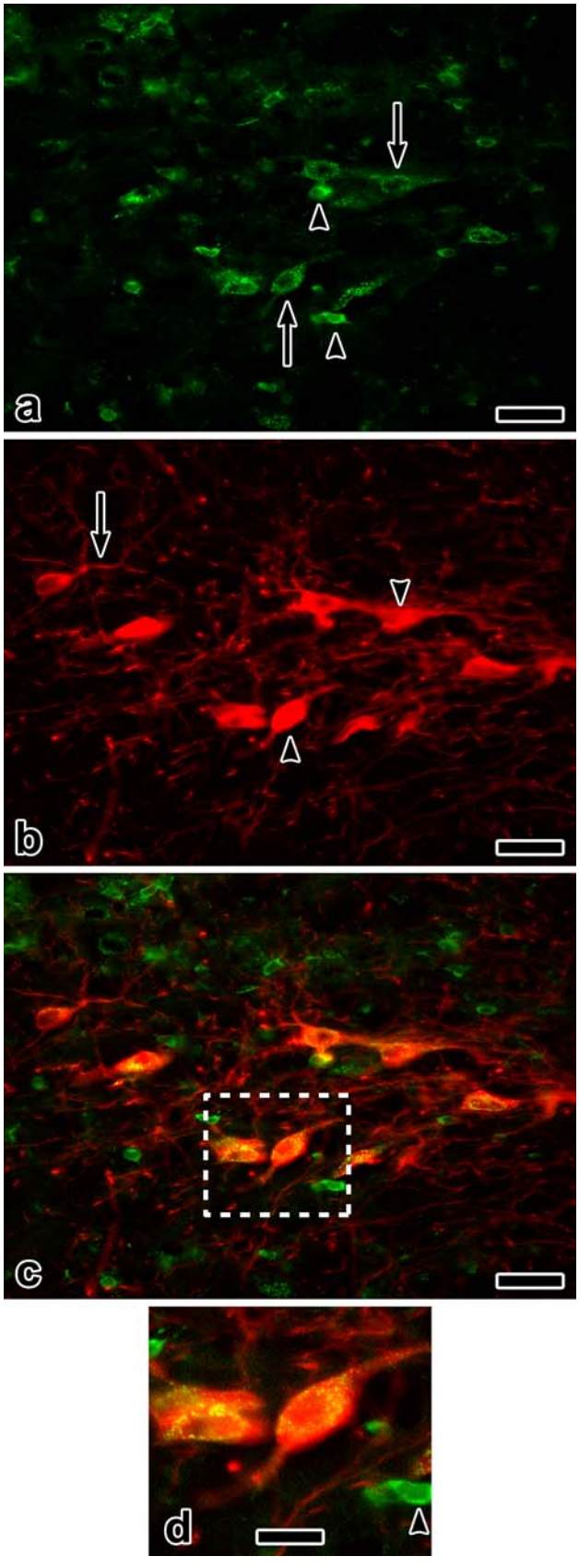

Fig. 3 Double staining of *KAT-I* and *TH* at the level of immune fluorescence. **a** *KAT-I IR* is located in the neurons of the *SNPC* (*arrows*) and in the glial cells (*arrowheads*) (scale bar, 30 μm). **b** *TH IR* is located exclusively in neurons (*arrows*); abundant neuronal processes are also *TH IR* (scale bar, 30 μm). **c** Superposition of the *KAT-I* and *TH* in the identical areas of the section. It is apparent that the neurons contain both *KAT-I* and *TH* (scale bar, 30 μm). **d** The area outlined in **c** with immersion optics. *Yellow rings* around the nuclei denote *KAT-I IR*. The glial cells exert only green fluorescence, indicating *KAT-I IR* (*arrowhead*) (scale bar, 15 μm)

Demonstration of immunoreactivity

Endogenous peroxidase was blocked with 2% H_2O_2 dissolved in methanol. Sections were processed according to the avidin–biotin system (Vectastain ABC Elite, Vector Laboratories, Burlingame, CA, USA); immunoreactivity was visualized with diaminobenzidine (DAB, Polysciences, Inc., Warrington, PA, USA), to which hydrogen peroxide had been added (3 μl of H_2O_2 to 10 ml of 0.05% DAB). Sections were mounted on gelatin-pretreated glass slides, dehydrated in a graded series of ethanol, and processed through carbol-xylene. Slides were coverslipped with Permount (Fisher, Fair Lawn, NJ, USA).

Demonstration of KAT-I

The sections were incubated overnight at room temperature in anti-KAT-I polyclonal antibody raised in rabbit against rat kidney KAT-I [29], (1:1,500), in 0.01 M pH 7.4 PBS, containing Triton X-100 and normal goat serum. This was followed by 90-min incubation in biotinylated anti-rabbit secondary antibody.

Also, TH was demonstrated by incubation at room temperature overnight in anti-TH monoclonal antibody (Sigma) diluted to 1:10,000 in 0.01 M PBS (pH 7.4) containing 0.3% Triton X-100 and normal goat serum. Sections were incubated for 90 min in biotinylated anti-mouse secondary antibody. For the demonstration of glial fibrillary acidic protein (GFAP), sections were incubated in anti-GFAP raised in mouse (Sigma), diluted to 1:400, at room temperature overnight, followed by a 90-min incubation in biotinylated anti-mouse secondary antibody.

Microglial cells were demonstrated with CD11b (Chemicon International, Inc., Temecula, CA, USA) anti-rat primary antibody raised in mouse in a dilution of 1:400 at room temperature overnight, followed by a 90-min incubation in biotinylated anti-mouse secondary antibody.

Specificity of the immunohistochemical reactions was assessed by the following treatments:

1. Omission of the first (specific) antiserum.
2. Use of normal rabbit (or mouse, resp.) serum instead of the specific antiserum.
3. Treatment according to the avidin–biotin complex method, from which one of the steps had been omitted.
4. Preabsorbtion of the specific antibody with pure rat kidney KAT at 4°C for 24 h.

None of these specimens has shown any reaction.

For double staining of KAT-I and TH (immunofluorescence technique), 30-μm cryostat sections of the SN were collected on precoated slides. Using the simultaneous method, KAT-I antiserum, raised in rabbit [29] (1:1,500), and TH antiserum, raised in sheep (Chemicon) 1:10,000, were used as primary antibodies at room temperature overnight. The secondary serum was a mixture of FITC-conjugated donkey anti-rabbit IgG and Rhodamin Red-conjugated donkey anti-sheep IgG (Jackson Immuno Research Laboratories, Bar Harbor, ME, USA) in a dilution of 1:200, for 2 h at room temperature. After three rinses in PBS, the sections were coverslipped with polyvinyl alcohol mounting medium (DABCO Antifading, Fluka Chemie GmbH, Buch, Germany).

The verification of immunoreaction specificity in the SNPC proved that after omission of TH antibody from the primary serum, the subsequent visualization with the secondary antisera did not result in the fluorescence normally characterizing the TH cells.

Also, double staining of KAT-I and CD11b (immunofluorescence technique) was performed on cryostat sections, collected on precoated slides. The simultaneous method was used: KAT-I antiserum, raised in rabbit (1:1,500), and CD11b antiserum (Chemicon), raised in mouse (1:400), were used as primary antibodies, at room temperature overnight. After rinsing in PBS, the sections were treated with biotinylated anti-mouse IgG (Vector) 1:200 for 90 min. Incubation was followed in a medium containing FITC-conjugated anti-rabbit IgG (Vector) and streptavidin-conjugated CY 3 (Jackson) in a dilution of 1:200, for 2 h.

Finally for the double staining of KAT-I and GFAP (immunofluorescence), KAT-I antiserum, raised in rabbit (1:1,500) and GFAP antiserum (Santa Cruz Biotechnology, Inc., Santa Cruz, CA, USA) raised in goat (1:500), were used as primary antibodies. The incubation was performed at room temperature overnight, followed by treatment in a secondary antibody containing FITC-conjugated donkey anti-rabbit IgG and Rhodamin Red-conjugated donkey anti-sheep IgG (1:200) for 2 h.

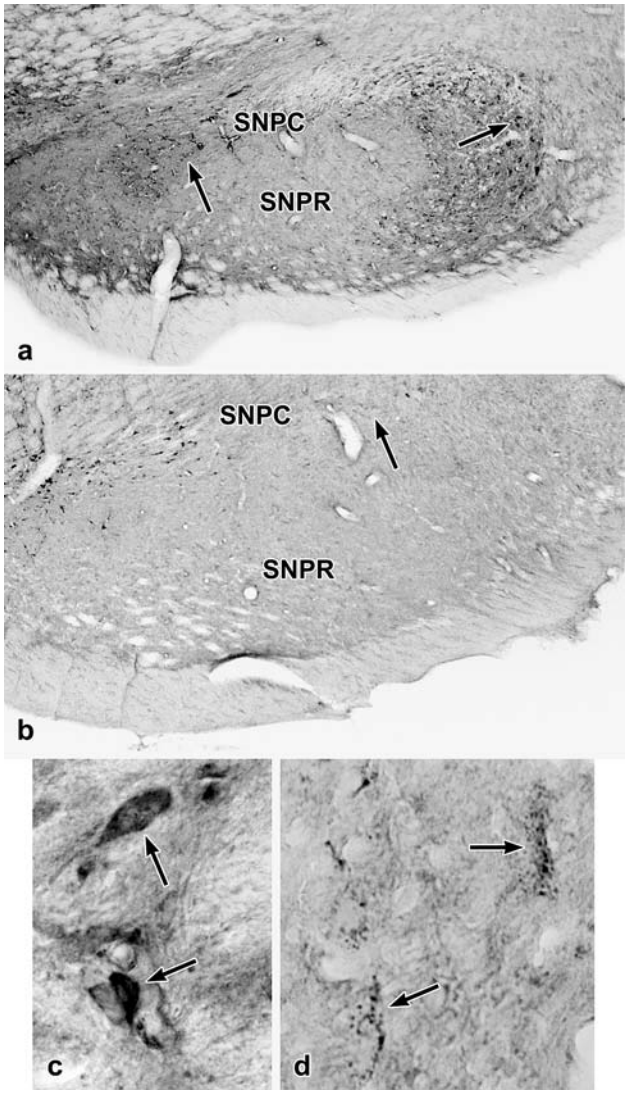

Fig. 4 Effects of 400 and 800 μg/kg of *6-OHDA*, 23 days after injection of the drug into the lateral ventricle. **a** Disappearance of *KAT-I IR*, mainly from the middle area of the *SNPC*, 23 days after treatment with 400 μg/kg of *6-OHDA* (*arrows*) (scale bar, 100 μm). **b** Disappearance of *KAT-I IR* from the middle and lateral areas of the *SNPC*, 23 days after treatment with 800 μg/kg *6-OHDA* (*arrow*) (scale bar, 100 μm). **c** Disorganization of *KAT-I IR* neurons, 23 days after treatment with 400 μg/kg of *6-OHDA*, at high power (*arrows*) (scale bar, 10 μm). **d** The shrinkage of the *KAT-I IR* neurons is striking 23 days after treatment with 800 μg/kg of *6-OHDA*, at high power (*arrows*) (scale bar, 10 μm)

Analysis of the fluorescent images and photography of the sections were performed using a Nikon Eclipse E600 microscope equipped with B-2A (EX: 450–490) and G-2A (EX: 510–560) filters and a Spot RT Slider digital camera (1,600 × 1,200 pixels in 24 bits). The software used was the Image Pro Plus 4.5 morphometry (Media Cybernetics, Silver Spring, MD, USA). The emitted fluorescence was determined by intensity measurement. We have been working with true color

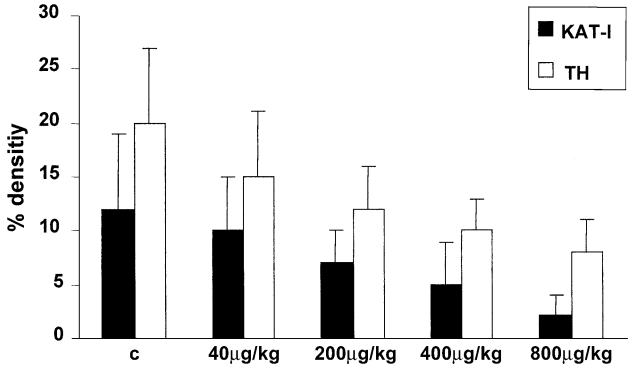

Fig. 5 Densitometric analysis of *KAT-I IR* and *TH IR* in the *SNPC* under normal conditions (C) and 23 days after *6-OHDA* treatment

images and, according to the quality of staining, we measured the luminosity of the green (for KAT-I IR cells) or the red (for TH, GFAP, and CD11b IR cells) channel. The analysis was performed in 6-6 randomly selected sections, in five areas of interest (AOI) in each group, using a 40× front lens (NA: 0.7). AOI was a rectangular box measuring 30 × 45 μm^2. In each measurement, we used a linear intensity scale; finally, the intensity of the black level was subtracted from the values obtained.

Electron microscopy

After transcardial PLP fixation, KAT-I and TH were visualized in vibratome sections (50 μm), using the same immunocytochemical procedures as employed for light microscopy, except that Triton X-100 was omitted from the incubation medium. After the DAB reaction, the sections were additionally fixed in buffered 1% osmic acid solution for 1 h. Following dehydration, the sections were flat-embedded on liquid

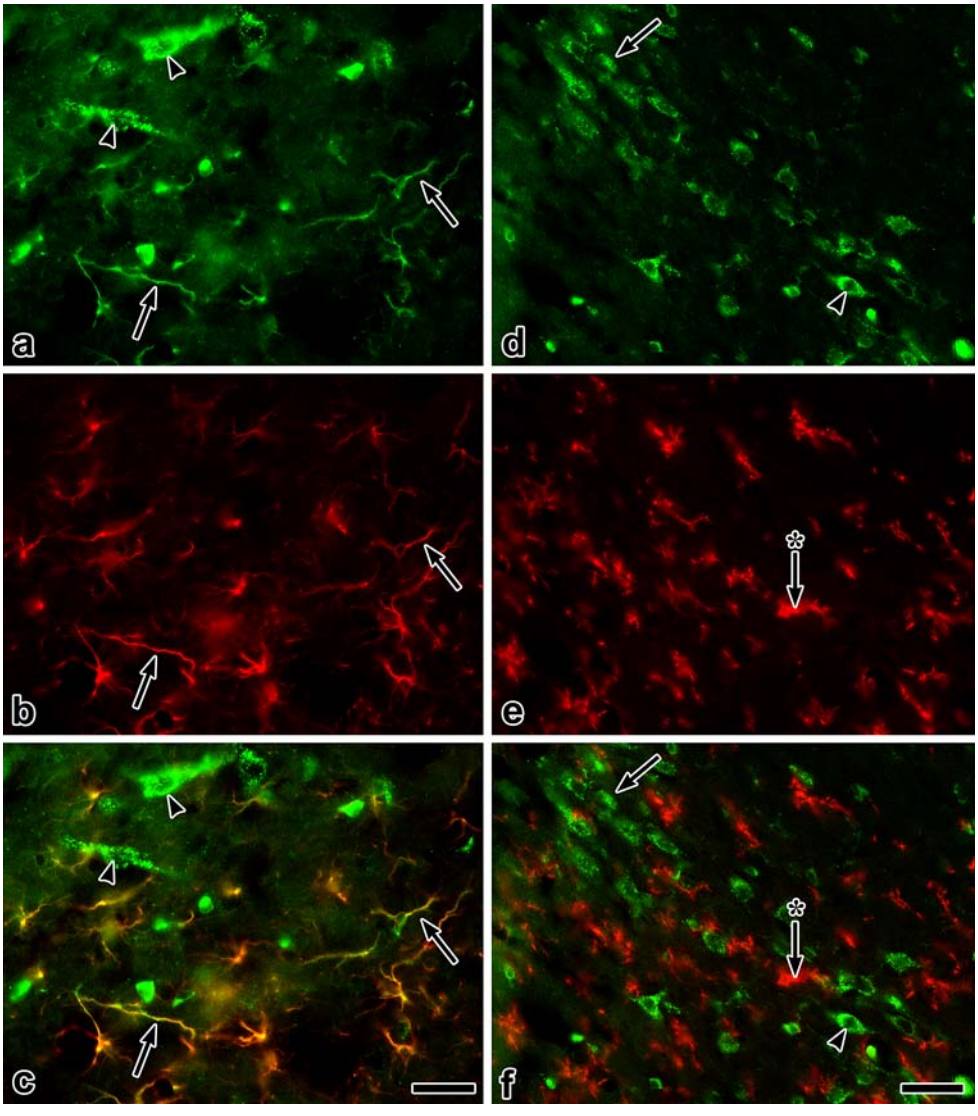

Fig. 6 Double staining of *KAT-I* and glial cell markers. **a** Astroglial cells (*arrows*) and neurons (*arrowheads*) exhibit *KAT-I IR* in the *SN* under normal conditions (scale bar, 200 μm). **b** Astroglial cells stained with the specific marker *GFAP* in the *SN* under normal conditions (*arrows*) (scale bar, 200 μm). **c** The superposition proves that the *KAT-I IR* and *GFAP IR* areas are identical (*arrows*). The neurons exert only *KAT-I IR* (*arrowheads*) (scale bar, 200 μm). **d–f** Double staining by *KAT-I* and the microglia-specific marker CD11b under normal conditions. **d** Only the neurons (*arrowhead*) and astroglial cells (*arrow*) exhibit *KAT-I IR* (scale bar, 30 μm). **e** Microglial cells stained by the specific marker CD11b (*arrow* with *asterisk*) (scale bar, 30 μm). **f** Superposition of *KAT-I* and CD11b *IR* in the same area. Microglial cells appear *red* (*arrow* with *asterisk*), whereas neurons (*arrowhead*) and astroglial cells (*arrow*) are *green* (scale bar, 30 μm)

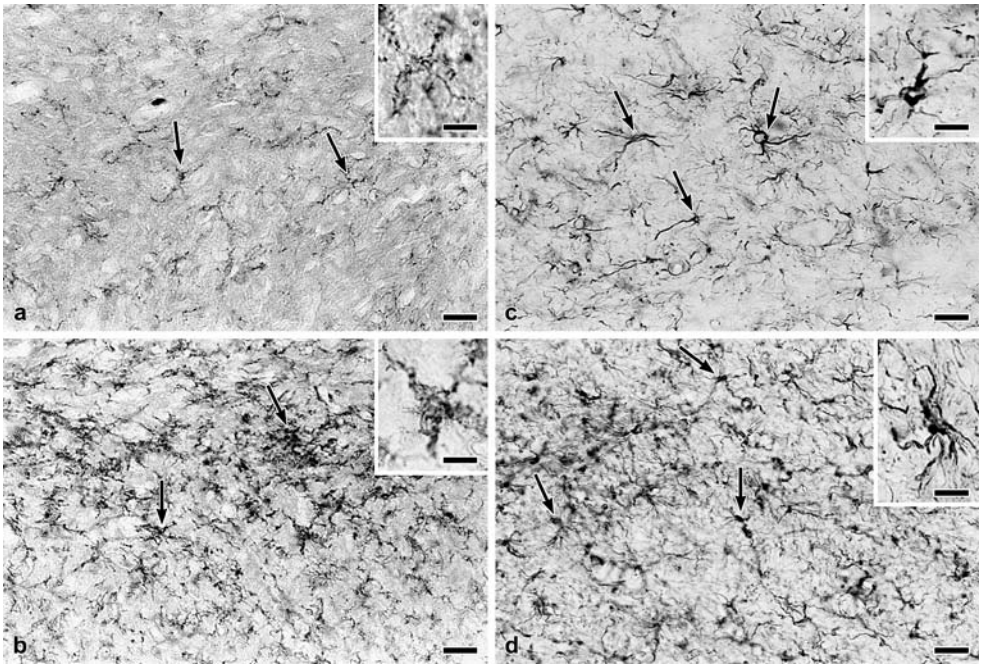

Fig. 7 Astroglial and microglial changes induced by *6-OHDA*. **a** Microglial cells (*arrows*) stained with the specific marker CD11b, using the ABC immunohistochemical technique. Normal control (scale bar, 40 μm). Inset: characteristic ramifications of one of the microglial cells (scale bar, 10 μm). **b** Twenty-three days after the injection of 800 μg/kg of *6-OHDA*, the number of microglial cells is markedly increased, especially in the *SNPC* (*arrows*). Staining with CD11b (scale bar, 40 μm). Inset: one of the swollen microglial cells, displaying thickened processes (scale bar, 10 μm). **c** Astrocytes (*arrows*) stained with the specific marker *GFAP*, using the ABC technique. Normal control (scale bar, 40 μm). In the inset, one of the astroglial cells is shown at higher power (scale bar, 10 μm). **d** Twenty-three days after the injection of 800 μg/kg of *6-OHDA*: the number of astrocytes is markedly increased, especially in the *SNPC*. *GFAP* staining (scale bar, 40 μm). In the inset, one of the astroglial cells, with increased ramification of the processes, is shown at higher power (scale bar, 10 μm)

release-pretreated slides in Durcupan ACM. Relevant areas were excised with a razor blade under light microscopic control, remounted to prepolymerized blocks, and sectioned on a Reichert Ultrotome equipped with a diamond knife. Serial sections of silver interference color were collected on copper slot grids and stained with uranyl acetate and lead citrate. The sections were analyzed with a Zeiss Opton 902 electron microscope.

Results

Neurons

Under normal conditions, KAT-I IR outlined SNPC (Fig. 1a). High-power investigation revealed that KAT-I IR was located in a granular form in the perinuclear cytoplasm and in the proximal parts of nerve cell processes (Fig. 1b and inset), as well as in glial cell bodies. TH IR exhibited a similar localization in neuronal cytoplasms, both in SNPC and in SNPR; TH IR was also present in numerous neuronal processes throughout almost the entire SN (Fig. 1c). At high magnification, it was evident that TH IR of neurons was diffuse (Fig. 1d and inset), in contrast to the granular localization of KAT-I. In accordance with the light microscopic studies, electron microscopy revealed that KAT-I IR was localized in granules scattered in the cytoplasm, preferentially around the nucleus. On the basis of their ultrastructural appearance, these granules corresponded to multivesicular bodies (Fig. 2a, a*). In contrast, TH IR was localized in the endoplasmic reticulum where the product of the IR was attached to the surfaces of ribosomes (Fig. 2b).

Co-localization of KAT-I and TH was proved by double staining at the level of fluorescence microscopy. KAT-I IR was, however, less intensely fluorescent than TH IR. Processes of TH IR neurons were TH-immunopositive (Fig. 3a–d); glial cells also exerted KAT-I (Fig. 3a, c, d). Twenty-three days after injection of 400 μg/kg 6-OHDA in the lateral ventricle, KAT-I IR disappeared mainly from the middle area of SNPC (Fig. 4a), while after injection of 800 μg/kg, KAT-I disappeared from both the middle and lateral areas of SNPC (Fig. 4b). Shrinkage and degradation of KAT-I IR neurons in SNPC was especially striking at higher magnification (Fig. 4c, d) Injection of 6-OHDA into

the lateral ventricle caused dose-dependent changes in the number, density (Fig. 5) and distribution of dopaminergic neurons in SNPC. Counterstaining with cresyl violet revealed that in animals treated with 40 g/kg 6-OHDA, 67 ± 5% of TH IR SNPC neurons survived neurotoxin treatment after 23 days without any visible sign of deterioration; the relevant percentage in animals treated with 200 g/kg 6-OHDA was 33 ± 6%, in animals treated with 400 g/kg 6-OHDA was 24 ± 6%, while in those treated with 800 g/kg 6-OHDA was 10 ± 3%.

Glia

Under normal conditions, astroglial cells in the SN showed KAT-I IR (Fig. 6a) which co-localized with GFAP (Fig. 6b, c). Neurons in the same specimens were visible in green color (Fig. 6a, c) indicating the presence of KAT-I. Microglial cells, however, identified with the specific microglia marker CD11b (Fig. 6e), did not show any KAT-I IR under normal conditions (Fig. 6d). After superposition of KAT-I and CD11b IR (Fig. 6f), neurons expressing KAT-I appeared in green color, while CD11b-stained microglia appeared in red color.

Immunohistochemical studies performed with the specific microglial marker CD11b (Fig. 7a) revealed that the number of microglial cells increased markedly 23 days after 800 µg/kg 6-OHDA treatment (Fig. 7b). At the same time, also the microglial processes have shown severe alterations (Fig. 7a, b, insets) insofar as microglial processes became more voluminous and elaborate.

Similar alterations were found in astrocytes stained with the specific astroglial marker GFAP: as compared with the controls (Fig. 7c and inset), the number of astroglial somata and processes increased considerably 23 days after 6-OHDA treatment (Fig. 7d and inset).

Densitometric analysis indicated that KAT-I IR increased significantly in glial cells of SNPC after 6-OHDA treatment, though the increase was far less striking than that of CD11b and GFAP, the specific markers of microglia and astroglia, respectively (Fig. 8a, b). This increase was probably due to clustering of glial cells—especially microglia—around affected neurons.

Electron microscopy revealed that, while some of the KAT-I IR granules characterizing SNPC neurons still existed 9 days after 40 µg/kg 6-OHDA treatment, large dense bodies indicating incipient degeneration appeared in the cytoplasms of nerve cells (Fig. 9a). Twenty-three days after 800 µg/kg 6-OHDA treatment, degenerating KAT-I IR nerve cells were characterized by shrinkage and darkening of the whole cell body; the perikaryon was surrounded by glial processes (Fig. 9b).

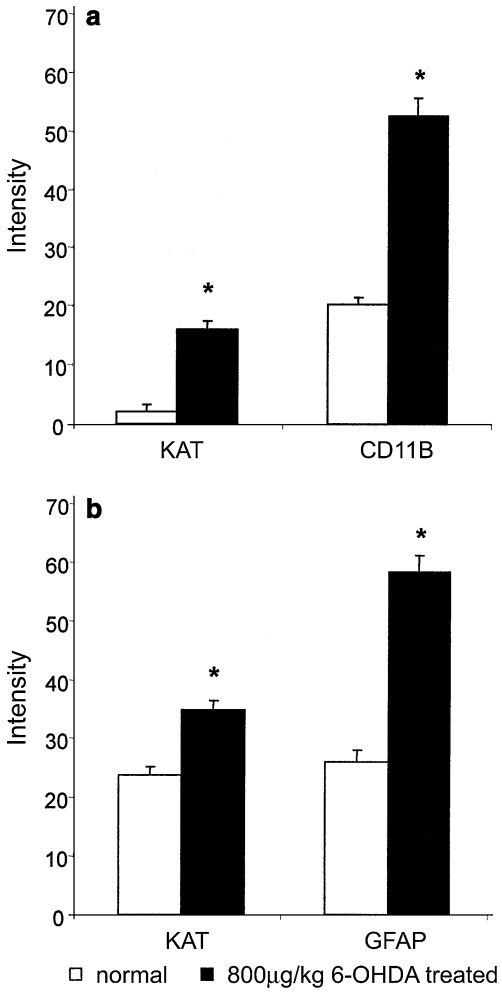

Fig. 8 Densitometric analysis of *KAT-I IR* and specific markers in glial cells in the *SN*. **a** Significant increase in *KAT-I IR* in the microglial cells 23 days after treatment with 800 µg/kg of *6-OHDA*, although the increase is far less than that in the specific microglia marker CD11b. **b** Significant increase in *KAT-I IR* in the astroglial cells 23 days after treatment with 800 µg/kg of *6-OHDA*, although the increase is less than that in the specific astroglial marker *GFAP*

Discussion

Animal models are still of use in facilitating an understanding of the neurodegeneration characteristics of PD. In the present paper, we have shown that unilateral injections of 6-OHDA into the lateral ventricle of the adult rat lead to a dose-dependent, gradual loss of TH and KAT-I from the SNPC. Intracerebroventricular administration [33] results in poor diffusion; nevertheless,

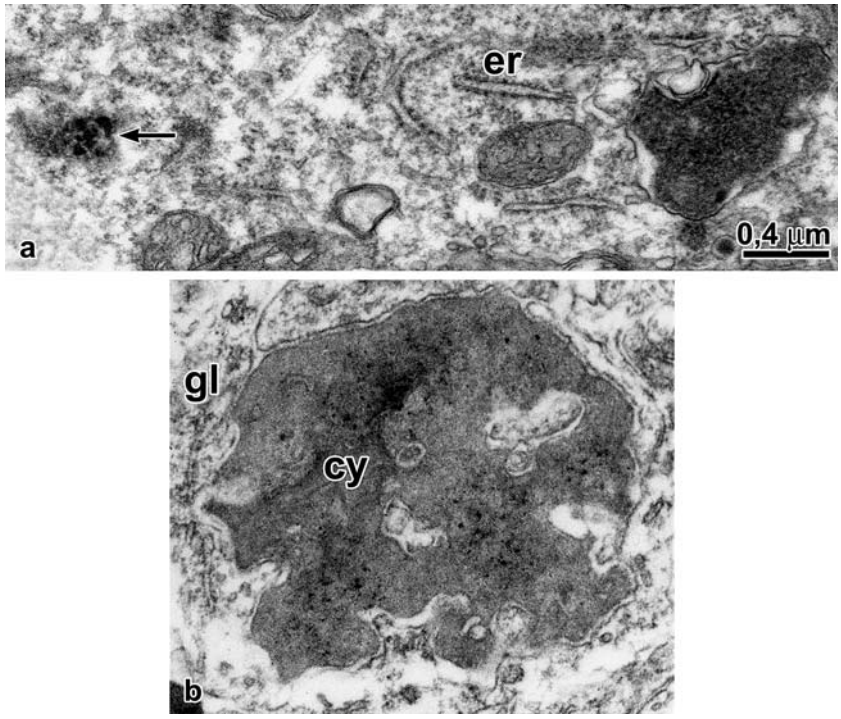

Fig. 9 Electron microscopy of *KAT-I IR* in degenerating nerve cells of the *SNPC*. **a** Portion of the cytoplasm of a *KAT-I IR* neuron 12 days after the injection of 40 µg/kg of *6-OHDA*. In spite of the presence of a few *KAT-I IR* granules (*arrow*), large degenerative dense bodies appear (*asterisk*). *er*: endoplasmic reticulum. **b** Remnants of a shrunken and darkened nerve cells in the *SNPC* 23 days after treatment with 800 µg/kg of *6-OHDA*. Residual *KAT-I IR* is marked with *asterisks*. Glial cell processes (*gl*) surround the debris of the cytoplasm (*cy*). The magnification is identical to that in **a**

in this way the retrograde degeneration of the parent cells located in the SN (commonly observed after injection into the striatum) can be avoided. At the highest dose of 6-OHDA that we employed (800 µg/kg), the TH and KAT-I IR of the nerve cells diminished considerably in the SNPC, either transiently or irreversibly, in consequence of cell death [23] or apoptosis [2, 24].

The presence of KAT-I (CCBL1 according to the HUGO nomenclature [8]) in the glial cells is a well-known fact [7, 22, 30]. To date, however, only certain neurons in the CNS have been shown to contain KAT-I [7, 18, 21, 22, 30, 32]. We report here on the presence of KAT-I in the SN neurons in the rat and its co-existence with TH, similarly as described earlier in the mouse [21].

After 6-OHDA treatment, the optical intensity of the specific markers GFAP and CD11b increased in the SNPC, due to the accumulation of astroglial and microglial cells. This observation is in accord with the results of Iravani et al. [16], who found that the loss of dopaminergic neurons from the SN in PD may result from the inflammation-induced proliferation of microglia and reactive macrophages, accompanied by intense GFAP IR astrocytosis in the SN. Similar increases in GFAP IR astrocytes and CD11b IR microglial cells were earlier observed [21] in the SN of mice after MPTP treatment. Under normal conditions, only the astrocytes contain KAT-I; however, after 6-OHDA treatment, the microglial cells also were found to be KAT-I IR, even though the amount of KAT-I was still larger in the astrocytes than in the microglial cells, probably because the astrocytes contained KAT-I even under normal conditions.

Although the origin of the KAT-I in the microglial cells after 6-OHDA treatment is unknown, it can be assumed that it is derived from internalized KAT-I immunopositive neurons. Guillemin et al. [10] concluded that astrocytes, which alone are neuroprotective, become indirectly neurotoxic in the presence of microglia, since microglial cells produce large amounts of kynurenine that can be metabolized to quinolinic acid. Quinolinic acid has recently been shown to induce chemokine production and chemokine receptor expression in the astrocytes [9].

Reactive astrocytes, or rather functionally activated astrocytes, have been observed in numerous 6-OHDA animal models of PD. Although the astrocytes have traditionally been assumed to impede neuronal regeneration, activated microglia and reactive astrocytes have been found in the area of neuronal loss [39]; these glial elements possibly contribute to the inflammatory process by releasing prostaglandins or cytokines, and may mediate neuroprotection by releasing trophic factors [3]. Recent studies indicate that reactive astrocytes may offer crucial benefit in the functional recovery from brain injuries: for instance, Vila et al. [40] suggest that the glial response may be the source of trophic factors protecting against glutamate and reactive oxygen compounds. Accordingly, Chen et al. [3] hypothesize that reactive astrocytes may play important roles in the protection of dopaminergic neurons in the SN. Ishida

et al. [17] suggest that the increased expression of protease-activated receptor-1 by the astrocytes in the SNPC provides neuroprotection during the progression of PD pathology. This is in line with our observation that the KAT-I IR of the astrocytes was increased after 6-OHDA treatment.

What is the role of KAT-I in the nigral neurons? Following the loss of dopamine, enhanced NMDA receptor-mediated synaptic transmission was detected in the striatum [26]; the situation may possibly be similar in the SN. On the other hand, excess glutamatergic transmission at NMDA receptors has recently been hypothesized to play a role in the expression of the symptomatology of PD [19]. In view of the neuroprotective role of KYNA synthesized by KAT-I, it may be assumed that KAT-I participates in an intrinsic, genuine defense mechanism, protecting the nigral dopaminergic neurons from the consequences of minor injuries occurring throughout life.

The content of KYNA in the SNPC neurons is apparently insufficient to protect them from the deleterious effect of 6-OHDA; however, ongoing neurobiological studies [27] may reveal new approaches to increase the amount of KYNA in the SNPC, and this, together with the glial contribution outlined above, might possibly provide neuroprotection and prevent the neuropathological consequences of PD.

Acknowledgments The authors thank Prof. Karoly Balogh (Department of Pathology, Beth Israel Deaconess Medical Center, Harvard Medical School, Boston, MA, USA) for editing the manuscript, Dr. Etsuo Okuno (Department of Molecular Medicine, Wakayama Medical University, Japan) for the KAT-I antibody, Mrs. Valeria Széll (Department of Neurology, University Medical School, Szeged, Hungary) for skillful histotechnical assistance, and Mr. Mihály Dezső (Department of Pathology, University Medical School, Szeged, Hungary) for the computerized photomicrographic work. This study was supported by the Hungarian Scientific Research Foundation (grants OTKA T-025033 and T-032039), the Hungarian Medical Research Foundation (grants ETT 007/2003, 9/2003, and 10/2003), BIO-O.M. (grant 00100/2002), and NKTH Szeged (grant 08/2004).

References

1. Barkats M, Millecamps S, Bilang-Bleuel A, Mallet J (2002) Neuronal transfer of the human Cu/Zn superoxide dismutase gene increases the resistance of dopaminergic neurons to 6-hydroxydopamine. J Neurochem 82:101–109
2. Blum D, Torch S, Lambeng N, Nissou M, Benabid AL, Sadoul R, Verna JM (2001) Molecular pathways involved in the neurotoxicity of 6-OHDA, dopamine and MPTP: contribution to the apoptotic theory in Parkinson's disease. Progr Neurobiol 65:135–172
3. Chen LW, Young KL, Chen YS (2005) Reactive astrocytes as potential manipulation targets in novel cell replacement therapy of Parkinson's disease. Curr Drug Targets 6:821–833
4. Choi DW, Rotman SM (1990) The role of glutamate neurotoxicity in hypoxic–ischemic neuronal death. Rev Neurosci 13:171–182
5. Csillik A, Knyihár-Csillik E, Okuno E, Krisztin-Péva B, Csillik B, Vécsei L (2002) Effect of 3-nitropropionic acid on kynurenine aminotransferase in the rat brain. Exp Neurol 177:233–241
6. Dauer W, Przedborski S (2003) Parkinson's disease: mechanisms and models. Neuron 39:889–909
7. Du F, Schmidt W, Okuno E, Kido R, Koehler C, Schwarz R (1992) Localization of kynurenine aminotransferase immunoreactivity in the rat hippocampus. J Comp Neurol 321:477–487
8. Eyre TA, Ducluzeau F, Sneddon TP, Povey S, Bruford EA, Lush MJ (2006) The HUGO gene nomenclature database, 2006 updates. Nucleic Acids Res 34:D319–D321
9. Fukuda T (2001) Neurotoxicity of MPTP. Neuropathology 21:323–332
10. Guillemin GJ, Smith DG, Kerr SJ, Smythe GA, Kapoor V, Armati PJ, Brew BJ (2000) Characterization of kynurenine pathway metabolism in human astrocytes and implications in neuropathogenesis. Redox Rep 5:108–111
11. Han Q, Li J, Li J (2004) pH dependence, substrate specificity and inhibition of human kynurenine aminotransferase I. Eur J Biochem 271:4804–4814
12. He Y, Lee T, Leong SK (2000) 6-Hydroxydopamine induced apoptosis of dopaminergic cells in the rat substantia nigra. Brain Res 858:163–166
13. He Y, Lee T, Leong SK (1999) Time-course and localization of transferrin receptor expression in the substantia nigra of 6-hydroxydopamine-induced Parkinsonian rats. Neuroscience 91:579–585
14. Hökfelt T, Ungerstedt U (1973) Specificity of 6-hydroxydopamine induced degeneration of central monoamine neurones: an electron and fluorescence microscopic study with special reference to intracerebral injection on the nigro-striatal dopamine system. Brain Res 60:269–297
15. Ichitani Y, Okamura H, Nakahara D, Nagatsu I, Ibata Y (1994) Biochemical and immunocytochemical changes induced by intrastriatal 6-hydroxydopamine injection in the rat nigrostriatal dopamine neuron system: evidence for cell death in the substantia nigra. Exp Neurol 130:269–278
16. Iravani MM, Kashefi K, Mander P, Rose S, Jenner P (2002) Involvement of inducible nitric oxide synthase in inflammation-induced dopaminergic neurodegeneration. Neuroscience 110:49–58
17. Ishida Y, Nagai A, Kobayashi S, Kim SU (2006) Upregulation of protease-activated receptor-1 in astrocytes in Parkinson disease: astrocyte-mediated neuroprotection through increased levels of glutathione peroxidase. J Neuropathol Exp Neurol 65:66–77
18. Kapoor R, Okuno E, Kido R, Kapoor V (1997) Immunolocalization of kynurenine aminotransferase (KAT) in the rat medulla and spinal cord. Neuroreport 16:3619–3623
19. Kelsey JE, Mague SD, Pijanowski RS, Harris RC, Kleckner NW, Matthews RT (2004) NMDA receptor antagonists ameliorate the stepping deficits produced by unilateral forebrain bundle injections of 6-OHDA in rats. Psychopharmacology 175:179–188
20. Kessler M, Terrama NI, Lynch G, Baudry M (1989) A glycine site associated with *N*-methyl-D-aspartic acid receptors: characterization and identification of a new class of antagonist. J Neurochem 52:1319–1328
21. Knyihár-Csillik E, Csillik B, Pakaski M, Krisztin-Péva B, Dobo E, Okuno E, Vécsei L (2004) Decreased expression of kynurenine aminotransferase-I (KAT-I) in the substantia

nigra of mice after 1-methyl-4-phenyl-1,2,3,6-tetrahydropyridine (MPTP) treatment. Neuroscience 126:899–914
22. Knyihár-Csillik E, Okuno E, Vécsei L (1999) Effects of in vivo sodium azide administration on the immunohistochemical localization of kynurenine aminotransferase in the rat brain. Neuroscience 94:269–277
23. Lee CS, Sauer H, Björklund A (1996) Dopaminergic neuronal degeneration and motor impairments following axon terminal lesion by intrastriatal 6-hydroxydopamine in the rat. Neuroscience 72:641–653
24. Marti MJ, Saura J, Burke RE, Jackson-Lewis V, Jimenez A, Bonastre M, Tolosa E (2002) Striatal 6-hydroxydopamine induces apoptosis of nigral neurons in the adult rat. Brain Res 958:185–191
25. McLean IW, Nakane PK (1974) Periodate-lysine-paraformaldehyde fixative: a new fixative for immunoelectron microscopy. J Histochem Cytochem 22:1077–1083
26. Nash JE, Brotchie JM (2002) Characterization of striatal NMDA receptors involved in the generation of Parkinsonian symptoms: intrastriatal microinjection studies in the 6-OHDA lesioned rat. Mov Disord 17:455–466
27. Nemeth H, Robotka H, Kis Z, Rozsa E, Janaky T, Somlai C, Marosi M, Farkas T, Toldi J, Vécsei L (2004) Kynurenine administered together with probenecid markedly inhibits pentyltetrazol-induced seizures: an electrophysiological and behavioral study. Neuropharmacology 47:916–925
28. Nozaki K, Beal MF (1992) Neuroprotective effect of L-kynurenine on hypoxia–ischemia and NMDA lesions in neonatal rats. J Cereb Blood Flow Metab 12:400–407
29. Okuno E, Du F, Ishikawa M, Tsujimoto M, Nakamura M, Schwarcz R, Kido R (1990) Purification and characterization of kynurenine-pyruvate aminotransferase from rat kidney and brain. Brain Res 354:37–44
30. Okuno E, Nakamura M, Schwarcz R (1991) Two kynurenine aminotransferases in human brain. Brain Res 542:307–312
31. Paxinos G, Watson C (1982) The rat brain in stereotoxic coordinates. Academic, Sydney, pp 56–57
32. Roberts RC, Du F, McCarthy KE, Okuno E, Schwarcz R (1992) Immunocytochemical localization of kynurenine aminotransferase in the rat striatum: a light and electron microscopic study. J Comp Neurol 326:82–90
33. Rosenblad C, Kirik D, Drevaux B, Moffat B, Phillips HS, Björklund A (1999) Protection and regeneration of nigral dopaminergic neurons by neurturin or GDNF in a partial lesion model of Parkinson's disease after administration into the striatum or the lateral ventricle. Eur J Neurosci 11:1554–1566
34. Sauer H, Oertel WH (1994) Progressive degeneration of nigrostriatal dopamine neurons following intrastriatal terminal lesions with 6-hydroxydopamine: a combined retrograde tracing and immunocytochemical study in the rat. Neuroscience 59:401–415
35. Schwarcz R, Pelliciari R (2002) Manipulation of brain kynurenines: glial targets, neuronal effects and clinical opportunities. J Pharmacol Exp Ther 303:1–10
36. Speciale C, Schwarcz R (1990) Uptake of kynurenine into rat brain slices. J Neurochem 54:156–163
37. Speciale C, Hares K, Schwarcz R, Brookes N (1989) High-affinity uptake of L-kynurenine by a Na^+-independent transporter of neutral amino acids in astrocytes. J Neurosci 9:2066–2072
38. Stone TW (1993) Neuropharmacology of quinolinic and kynurenic acids. Pharmacol Rev 45:309–379
39. Teismann P, Schulz JB (2004) Cellular pathology of Parkinson's disease: astrocytes, microglia and inflammation. Cell Tissue Res 318:149–161
40. Vila M, Jackson-Lewis V, Guegan C, Wu DC, Teismann P, Choi DK, Tieu K, Przedborski S (2001) The role of glial cells in Parkinson's disease. Curr Opin Neurol 14:483–489